

STUDIES ON FIRE-INDUCED VIBRATION OF FULL-SCALE CONTINUOUS PANELS USING HILBERT TRANSFORM

B. Li¹ – Y.L. Dong^{1,2*}

¹School of Civil Engineering, Harbin Institute of Technology, Huang he Road 73, Harbin, China, 150090

²College of Civil Engineering, Huaqiao University, Xiamen, China, 361021

ARTICLE INFO

Article history:

Received: 14.10.2013.

Received in revised form: 15.11.2013.

Accepted: 09.12.2013.

Keywords:

Fire test

Thermal vibration

Acceleration signals

Frequency

Boundary constraints

Hilbert Transform

Abstract:

Fire-induced vibration of four panels A-D has been studied and also relevant furnace temperature, temperature gradient, deflections and cracking distributions introduced. Time-domain analysis indicating vibration intensity has important relationships with boundary constraints. According to vibration intensity, the whole vibration process can be divided into three stages. During the first and third stages, acceleration signals are relatively low but during the second stage, vibration signals are strong so that more signal mutations have been detected. The signal mutations are due to the appearance of the main cracks. Frequency-domain analysis adopting Hilbert Transform (HT) shows that frequencies have been affected by cracks propagation and boundary constraints but the changes have not been influenced by damage locations in each panel. Furthermore, frequencies have fluctuated little in the first stage, but during the second stage, frequencies have fluctuated dramatically as a result of cracking propagations and an obvious falling trend has appeared. Also, in this stage frequencies have increased as a result of temporary swelling and increased friction within the panels. In the third stage, frequencies have changed smoothly and declined quickly. Moreover, the three stages of frequency changes correspond to the three stages of deflection changes in sequence. Therefore, characteristics of fire behaviour including deformation and cracks of the panels can be monitored through analysis of vibration.

1 Introduction

The vibration-based method has been developed in

the past few years and widely used in civil, mechanical and aerospace engineering for monitoring structural condition and for identifying

* Corresponding author. Tel.: (+86)15846592057

E-mail address: dongyl1965@163.com (Y.L. Dong); tingchao136@gmail.com

structural damage [1-7]. However, the application of the method in order to receive the real vibration parameters of civil engineering structure is still a challenging research topic due to its large dimensions and associated uncertainty. At present, relevant studies mainly focus on developing both advanced algorithm [2-3] and real time data acquisition system [1]. Furthermore, the vast majority of published work about the effect of changing temperature on vibration characteristics of civil engineering structures has mainly considered environmental temperature changes due to seasonal weather or radiation from sunshine [4-6], among which the ones by Rohrman and Rucker [8-9] concluded that vibration frequencies are decreased by increasing the temperature. Xia et al. [4] pointed out that the frequencies are decreased while the damping ratios are increased consistently with an increase in temperature and humidity, whereas the mode shapes are insensitive to the temperature and humidity change. Xu and Wu [5] studied the effects of change in environmental temperature on the frequencies and mode shape curvatures of a cable-stayed bridge, and changes obtained in dynamic characteristics of the bridge due to damage in girders or cables may be smaller than changes in dynamic characteristics due to variations in temperature. Peeters et al. [6] demonstrated the undeniable effect of temperature on measured eigenfrequencies and proposed a methodology for distinguishing temperature effect from real damage events. Apparently, these studies have mainly considered the ambient temperature effect on the civil engineering structures. However, the effect of elevated temperature on structural vibration has hardly been involved.

As serious structure fires occur more and more frequently, techniques used for monitoring burning structures and providing relevant damage prediction are receiving increasing attention. Fire-induced vibration health monitoring was first demonstrated in a test conducted on a single-family wood frame structure in Kinston, North Carolina (August 2001) [10]. The fire test for the first time showed that fire is capable of exciting dynamic structural vibration response providing real-time indication of impending collapse. In order to test the latest fire-sensor technology, a series of wood frame (or simple frame) burn tests were conducted. At last, the Health of Burning Structures (HOBS) Panel was established to track the structure's behaviour from

ignition to collapse [11]. Due to current limitation in numerical simulation, structural dynamics studies under fire mainly rely on expensive tests to provide recommendation on specific problems. Since relevant papers are poor, further studies need to be proceeded. This paper presents fire-induced thermal vibration of the continuous panels A-D in a full-scaled steel-framed building and investigates relevant vibration signals through time-domain and frequency-domain analysis.

2 Testing building

The building itself was described in several other papers [12, 14]. As a normal reinforced concrete floor shown in Fig. 1 and 2, the floor slab is 120 mm in depth and is made of grade 30 normal-weight concrete.

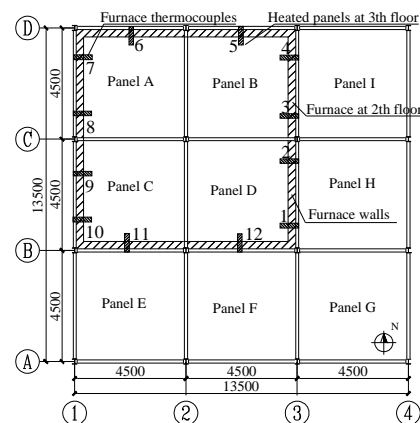


Figure 1. Location of test panels under fire.

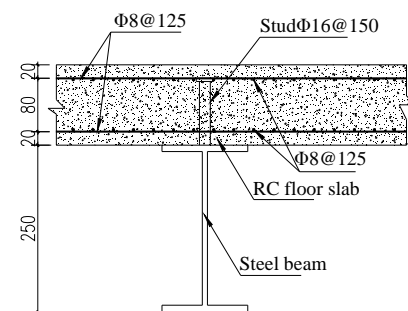


Figure 2. Cross-section of composite beam.

The hot-rolled reinforced bars are 8mm in diameter with 20 mm protective coating. The sections of steel beams and steel columns constructed from Q235 steel (Yield Strength 235 MPa) are H250×125×6×9 and H200×200×8×12, respectively. Composite

beam behaviour is achieved through the shear studs to connect steel beams and concrete slabs. The testing panels are located on the third floor of the building between the grid line B to D and 1 to 4 with an area of 9 m long and 9 m wide (Fig. 1). In order to report the experimental results easily, the continuous panels, as shown in Fig. 1, are named by panel A to I, orderly. The whole vibration data acquisition system includes vibration sensors (Fig. 4), the signal amplifier and relevant data collecting software. During the test, vibration sensors are installed on the firebricks which are bonded on the upper surface of the central area of each heated panel with cement mortar. Meanwhile, the sensors have been protected by mineral wool. In this way, they are secured and keep in touch with the top surface of panels to maintain synchronization.

3 Furnace

A furnace is specially designed and built beneath the test slab so that the test slab itself is a part of the closed furnace. As shown in Fig. 3, the four side furnace walls are constructed from red bricks consisting of outer walls (240 mm deep), interbedding mineral wool layer (50 mm deep) and inner walls (120 mm deep), sequentially. The gap between the top furnace walls and test slab is filled with mineral wool not only to keep the test components deforming freely but also to reduce heat loss. The columns and beam-to-column connections within the furnace are fully protected to keep the stability of the structure, while the beams in the furnace are subjected to fire directly without protection. The beams and columns on the perimeter of the furnace are almost insulated from fire. The furnace is operated with sixteen diesel oil-fired burner nozzles located in the furnace walls and each nozzle is controlled independently.

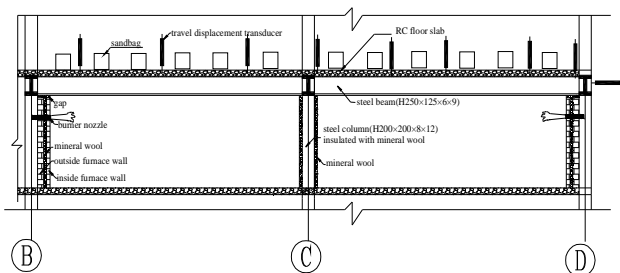


Figure 3. Elevation view of the furnace.



Figure 4. Arrangement of vibration sensors.

4 Thermal response

Test observations indicating changes of a vibration signal are related with deflection changes and cracking propagations. Thus, in this paper the furnace temperature, temperature gradient along the depth, deflection measurements as well as cracking distributions are introduced to describe the thermal vibration easily.

4.1 The furnace temperature

Fig. 3 shows the average furnace temperature plotted as a function of time, measured by twelve thermocouples (numbered 1-12 as shown in Fig. 1) within the furnace. When the furnace is shut off at 290 min, the average temperature reaches about 780 °C. The temperatures measured by thermocouples 2 and 9 are also plotted in the figure in order to reflect the uniformity of the furnace temperature so that the furnace temperature can fulfill the requirement of the fire test. Clearly, the fire is characterized by the heating-up phase and the cooling-down phase. It should be pointed out that the paper is only concerned with frequency changes during the heating-up phase.

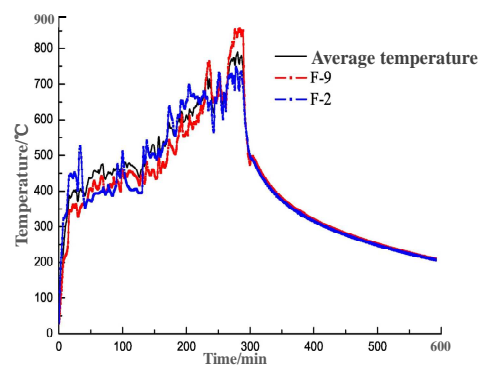


Figure 5. Recorded furnace gas temperatures.

4.2 Temperature gradient

Data processing shows temperature profiles along the depth of panels A-D that are similar. Therefore, a measure point named A-2 (as shown in Fig. 6) is chosen to analyze the temperature field along its depth. Fig. 7 (A-2-1 to A-2-5) indicates temperature-time response at depth of 0mm (bottom surface), 30 mm, 60 mm, 90 mm and 120 mm (upper surface) of the measure point A. Obviously, these profiles change in similar trends, but the temperature plateau at about 100 °C, owing to the evaporation of moisture, shows significant differences in time and duration occurrence.

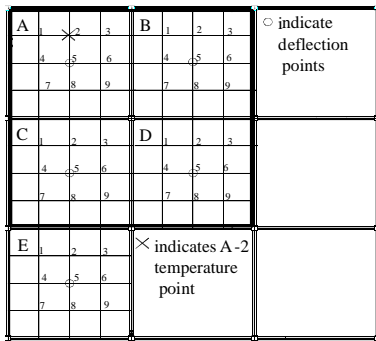


Figure 6. Arrangement of measure points.

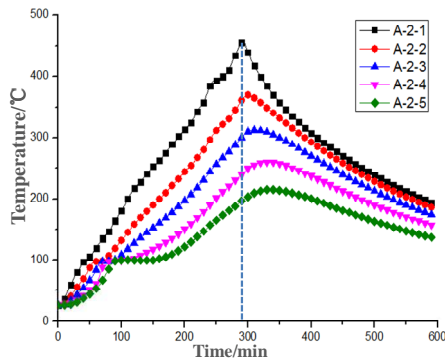


Figure 7. Temperature distributions along the depth.

4.3 Deflection analysis

Fig. 8 shows the vertical deflections at central part of each panel plotted as a function of time. Central deflections of panels A-D under fire indicate similar trends, but deflections of unheated panel E have been kept constant during the fire test. Additionally, there is a clear plateau at each deflection-time curve

of panels A-D during the heating-up phase, and the duration of the plateaus is 30, 60, 90 and 95 min, respectively. These curves also indicate that stronger boundary restraint leads to longer plateau duration. Finally, the mid-span vertical deflections of panels A-D, when the furnace is shut off, reach 180, 138, 110 and 127 mm, respectively. During the cooling-down stage, data from the LVDT at A-5 is not presented because the LVDT is found to be malfunctioning. According to deformation rate, each deflection curve during the whole heating-up stage can be divided into three stages. In the first stage, deflection increases slowly; in the medium stage, deflection increases relatively fast, but during its initial time, the displacement plateaus appear due to stiffening; in the late stage, deflection increase behaves faster.

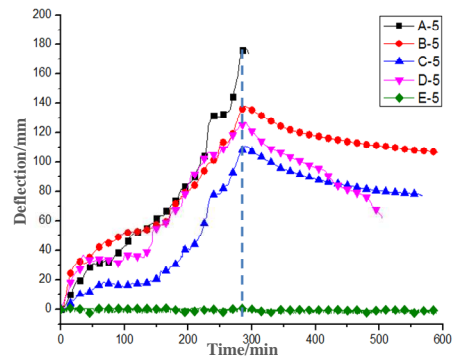


Figure 8. Vertical deflection at central part of each panel.

4.4 Cracking propagation

The major crack distributions were recorded during the fire test as shown in Fig. 9.

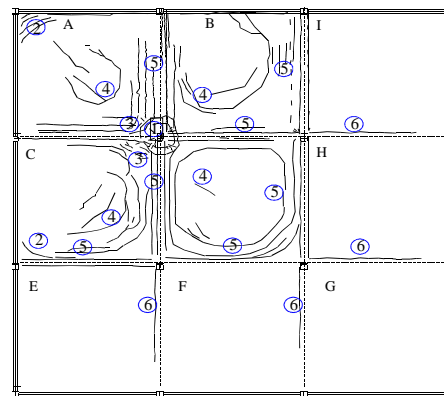


Figure 9. Crack pattern on the top of panels.

Several minutes after ignition, many circle cracks (denoted (1)) appeared around the column within furnace. At about 30 min, some arc cracks (denoted (2)) occurred, in the meantime, cracks (3) began to appear and spread quickly. These cracks are attributed to single point restraints of steel columns. Several minutes later, the arc cracks (3) appeared near the centre of each heated panel, and then some diagonal cracks (4) emerged and extended quickly. Meanwhile, the major cracks (5) developed along the full span of the panel and the maximum cracking width reached 10 mm. As heating continues, more and more cracks appeared on the four heated panels and extended towards the central area of the four panels, and eventually three types of cracking pattern were formed on the four panels [12].

5 Fire-induced vibration analysis of panels

At upper surface of the central area of each heated panel, an acceleration transducer is installed to gather structural vibration response. Four segments of the measured fire-induced vibration response acquired during the heating-up phase are shown in Fig. 10. Correlation analysis indicates that each segment of signal has no correlation with others.

5.1 Time-domain analysis

Fig. 10 a) shows the acceleration changes-time curve of panels A and the curve indicates that the whole vibration curves can be divided into three stages. The first stage lasts about 40 min and during the period a large transient response is produced as a result of an appearance of cracks (4). Due to bigger thermal inertia of concrete, the temperature of the panels A rises slowly although the furnace temperature rises very fast. Since the additional thermal strain is low, tiny cracks (1), (2) and (3) mostly appear. Correspondingly, the vibration amplitude is small and stable. The second stage lasts about 200 min, and in this stage, temperature rises very rapidly and temperature gradient along the depth of panel A becomes larger and larger, which leads to larger additional thermal strain and acceleration amplitude. Cracks (4), (5) propagate rapidly and maximum cracking width reaches even 10 mm, which produces many large transient signals. In comparison with the first stage, this stage shows high-level vibration characteristics and

produces lots of large transient responses at some time points. The third stage lasts about 50 min. During this stage, development of cracks (4), (5) is serious so that apparently the whole stiffness weakens. Meanwhile, as the thermal strain is relatively small, vibration amplitudes become low and large transient responses are hardly excited. Fire-induced acceleration versus time curves of panels B and C can also be divided into three stages. Compared with vibration response of panel A, the overall trend of vibration signals is similar. But during the first stage, the signal intensity is relatively low due to stronger boundary constraints and during the follow-up stage signal mutations increase apparently due to relatively dense cracks appearing in panels B and C.

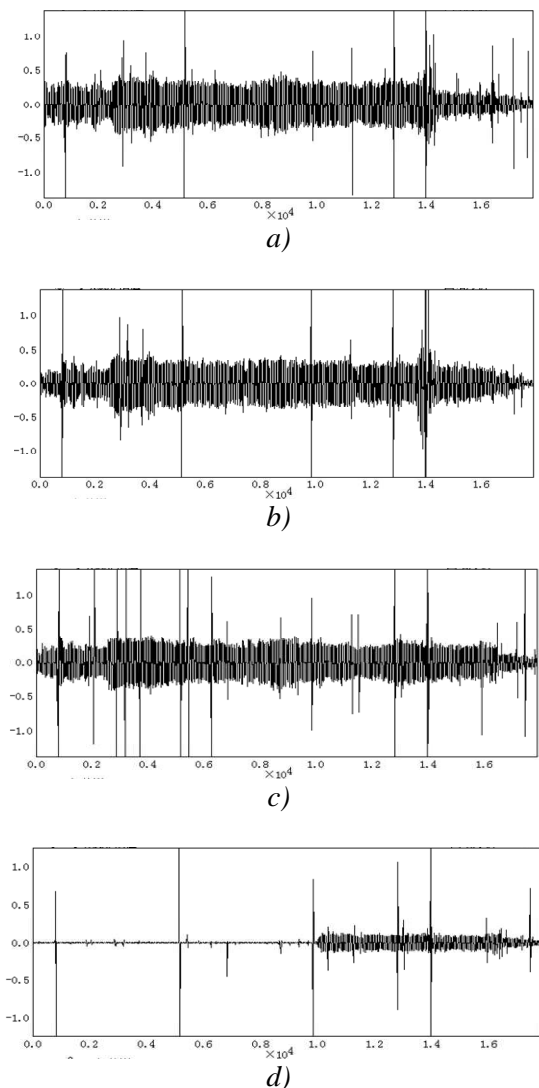


Figure 10. Time-history curves of acceleration.

Cracks can be therefore found to be the key factors for inciting signal mutations during the fire test. Data statistics shows that acceleration jumping has appeared 12 times in panel A, 8 times in panel B, 15 times in panel C and only 7 times in panel D. Furthermore, times of acceleration jumping at each acceleration vibration curve are mostly the same. This reflects that the powerful vibration signals can be transmitted within the four panels and are captured by the four sensors.

5.2 Frequency-domain analysis

Many damage detection methods use various transformations of measured signals such as Fourier transformation, Wavelet transform etc. The Fourier transformation is based on the basic functions group, $\sin()$ and $\cos()$, limiting thus the analysis of non-stationary signals. Wavelet transform can deal with the non-stationary signals but it is complicated to be adopted to extract continuous frequency [13]. Accordingly, previously published research using [11] Hilbert Transform (HT) can be employed as an effective method for extracting instantaneous frequency of engineering structures. Therefore, making use of the extracted frequency-time curves, reduced stiffness of the damaged panels due to fire can be obtained.

5.2.1 Mathematical background

HT is commonly introduced and defined through an improper integral [15]. To begin with, analytic signal $w(t)$ is introduced to be regarded as the HT of the impulse function $x(t)$. Then

$$w(t) = x(t) + jHT(x(t)). \quad (1)$$

The expression for the complex signal can be re-written using polar notation

$$w(t) = X(t)e^{jw_n(t)}, \quad (2)$$

where $X(t) = \sqrt{(x(t))^2 + (HT(x(t)))^2}$ and

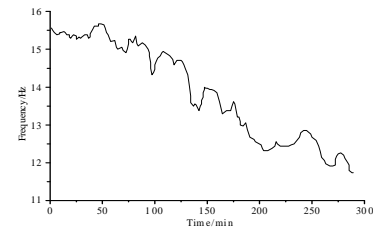
$w_n(t) = \text{Tan}^{-1}(HT(x(t))/x(t))$. Through above formulas the instantaneous frequency response can then be computed as the rate of change with respect to time of the phase response as

$$\text{Freq}(t) = d(w_n(t))/dt \quad (3)$$

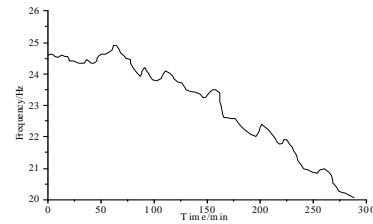
to produce an indicator that tracks the change in frequency behaviour as the structure burns.

5.2.2 Frequency-domain analysis via HT

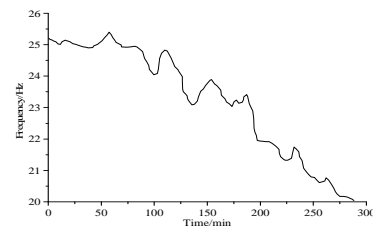
This paper analyzes the application of the HT, and the instantaneous frequency of each panel as a function of time is plotted through the heating-up phase. Fig. 9 shows significance of these results lying in remarkably smooth and decreasing trends in frequency.



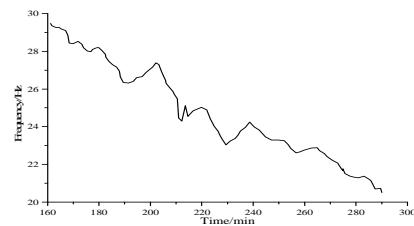
a)



b)



c)



d)

Figure 11. Frequency variation of panels.

Fig. 11 a) shows that changes of vibration frequency can also be divided into three stages, which coincide with the three stages, as mentioned above, divided according to the signal intensity. During the first stage, frequency fluctuations are small and the initial frequency reaches 15.6 Hz. In the second stage, the frequency values are quickly decreased and fluctuated in comparison with that of the first stage. It needs to be emphasized that there is a clear increasing portion at the beginning. Frequency increases are normally associated with stiffening behaviour, and this type of behaviour could be associated with temporary swelling and increased friction at critical connections within the structure. During the third stage, the frequency values are dropped more quickly due to severe cracking propagations and fast increasing of central deflection. The measurable decrease of instantaneous frequency during the heating-up stage reaches about 4 Hz, thus the residual stiffness is still relative large. Fig. 11 b) and c) shows similar trends of frequency changes compared with that of the panel A, but their frequency values are larger due to stronger boundary constraints. Furthermore, the two frequency-time curves can also be divided into three stages, and the maximum frequency occurs at about 60 min after ignition due to the stiffening effect. Fig. 11 d) shows the frequency changes of the panel D as a function of time from 160 min to 300 min. During the early stage (from 0 min to 160 min) fire-induced acceleration signals are very weak due to strong boundary constraints of panel D, thus the data gathered cannot provide useful information of the panel. From 160 min to 265 min, the frequency values vary dramatically from 29.5 Hz to 22.7 Hz, in this period, frequency values fluctuate dramatically. At the end of the test, frequency values drop more quickly. According to the above analysis, frequencies of the panels A-D under fire change dramatically and show a downward trend. The detailed frequency

changes during the heating-up stage are shown in Table 1. From Table 1, it can be found that frequency values have a close relation with the boundary constraints, and when the constraints are stronger, the frequency values of the panels are larger. It needs to be emphasized that during the first stage, the panel D hardly generated any vibration signals until some major cracks (5) greatly occurred. Combined with Fig. 8, it can be found that the three stages of frequency changes approximately correspond to the three stages of deflection changes in sequence. In the first stage, thermal expansion and temperature gradient of the panels are relatively low and many tiny cracks occur and propagate gradually, so frequency values are basically constant and vertical deflections increase slowly. In the second stage, cracking developments of panels are rapid and vibration signals are strong so that many signal mutations appear. Correspondingly, there are significant frequency changes and deflection changes are accelerated. In the third stage, material properties of the burned panels degenerate seriously and crack propagations show a smooth trend so that frequencies of panels are decreased more quickly and the rate of deflection changes improved. As fire continues to burn and weakening conditions develop, the panels soften in a manner consistent with the decreasing frequency behaviour. The last frequency values indicate that residual stiffness is still large. The fire-resisted performance is thus still strong despite the fact that the central maximum deflection of panels reaches 180 mm.

6 Conclusion

In this paper the fire-induced vibration response is investigated through time-domain analysis and frequency-domain analysis.

Table 1. Frequency changes of panels A-D.

Number	The first stage		The second stage		The third stage	
	Duration [min]	Frequency time [Hz]	Duration [min]	Frequency time [Hz]	Duration [min]	Frequency time [Hz]
Panel A	0-40	15.6-15.3	40-240	15.7-12.3	240-290	12.8-11.6
Panel B	0-45	24.6-24.4	45-225	24.9-22	225-290	22.4-20.7
Panel C	0-40	25.2-25	40-225	25.4-21.3	225-290	21.7-20.1
Panel D	0-160	-	160-230	29.5-23	230-290	24.2-20.1

Based on relevant results of this study, the following conclusions are drawn:

- 1) Continuous panels under fire can produce obvious vibration. The vibration process can be divided into three stages according to the intensity of vibration, and the intensity of vibration has important relationships with the boundary constraints of panels. When the constraints are stronger, the collected signal intensity is weaker.
- 2) Cracks propagations lead to mutations of thermal vibration signals of panels. As the cracks extend gradually, boundary constraints weaken accordingly. The frequencies are affected by cracks propagation and boundary constraints, but the changes are not influenced by damage locations in each panel. In the first stage, frequency values are basically constant. In the second stage, frequencies fluctuate dramatically as a result of cracking propagation. During their initial time, increases in frequency are normally due to stiffening structural behaviour; this behaviour should be associated with the temporary swelling and increased friction within the continuous panels. In the third stage, frequencies change smoothly and decline quickly. Thus, there is a significant difference between the ambient temperature and elevated temperature involving frequency changes compared with reference [4]. During the heat-up phase, frequency changes show a significant decreasing trend under fire.
- 3) Frequency changes mainly undergo three stages as listed in Table 1; this corresponds to the relevant stages of deflection changes and cracking propagations. Therefore, the fire behaviour of the panels can be monitored through the frequency analysis.

Acknowledgments

This research is supported by the NSFC with Grant No. 51178143. The authors gratefully appreciate the support.

References

- [1] Straser, E. G.: *A modular, wireless damage monitoring system for structures*, PhD thesis, Stanford University, USA, 1998.
- [2] Sohn, H., Farrar, C. R.: *Damage diagnosis using time series analysis of vibration signals*, Smart Material Structures, 10 (2001), 446-451.
- [3] Nair, K. K., Kiremidjian, A. S., Law, K. H.: *Time series-based damage detection and localization algorithm with application to the ASCE benchmark structure*, Journal of Sound and Vibration, 291 (2006), 349-368.
- [4] Xia, Y., Hao, H., Zanardo, G., Deeks, A.: *Long term vibration monitoring of RC slab: Temperature and humidity effect*. Engineering Structures, 28 (2006), 441-452.
- [5] Xu, Z. D., Wu, Z. S.: *Simulation of the effect of temperature variation on damage detection in a long-span cable-stayed bridge*, SHM, 6 (2007), 3, 177-189.
- [6] Peeters, B., Maeck, J., De Roeck, G.: *Vibration-based damage detection in civil engineering: Excitation sources and temperature effects*. Smart Material and Structures, 10 (2001), 518-527.
- [7] Volkovas, V., Eidukevičiute, M., Nogay, H. S., Akinci, T. C.: *Application of wavelet transform to defect detection of building's structures*, Mechanika, 18 (2012), 6, 683-690.
- [8] Rohrmann, R. G., Rucker, W. F.: *Surveillance of structural properties of large bridges using dynamic methods*, In: Proceedings of 6th international conference on structural safety and reliability, 1994, 977-980.
- [9] Rucker, W. F., Said, S., Rohrmann, R. G., Schmid, W.: *Load and condition monitoring of a highway bridge in a continuous manner*. In: Proceedings of the IABSE symposium on extending the lifespan of structures, 1995, 73.
- [10] Duron, Z. H., Ziyad, H. D.: *Early warning capacity for firefighters*. Testing of Collapse Prediction Techniques, NIST Report GCR, 16 (2003), 3, 846-857.